http://dx.doi.org/10.1016/j.bbamem.2015.03.009

The mitochondrial transporter of ascorbic acid functions with high affinity in the presence of low millimolar concentrations of sodium and in the absence of calcium and magnesium

Mara Fiorani[a], Catia Azzolini[a], Liana Cerioni[a], Maddalena Scotti[a], Andrea Guidarelli[a], Caterina Ciacci[b] and Orazio Cantoni[a,*]

[a]Dipartimento di Scienze Biomolecolari, Università degli Studi di Urbino "Carlo Bo", 61029 Urbino, Italy

[b]Dipartimento di Scienze della Terra, della Vita e dell'Ambiente, Università degli Studi di Urbino "Carlo Bo", 61029 Urbino, Italy

[*]*Corresponding author:* Prof. Orazio Cantoni, Dipartimento di Scienze Biomolecolari Università degli Studi di Urbino "Carlo Bo", 61029 Urbino, Italy. Tel: +39-0722-303523; Fax: +39-0722-303521. *E-mail address*: orazio.cantoni@uniurb.it

Abbreviations used: AA, L-ascorbic acid; DHA, dehydroascorbic acid; EB, extracellular buffer; IB, intracellular buffer; MB, mitochondrial buffer; SVCT, sodium-AA co-transporter.

Abstract

We recently reported that U937 cell mitochondria express a functional Na^+-dependent ascorbic acid (AA) transporter recognised by anti-SVCT2 antibodies. The present study confirms and extends these observations by showing that this transporter is characterised by a Km and a pH-dependence comparable with that reported for the plasma membrane SVCT2. In isolated mitochondria, Na^+ increased AA transport rate in a cooperative manner, revealed by a sigmoid curve and a Hill coefficient of 2, as also observed in intact Raw 264.7 cells (uniquely expressing SVCT2). There was however a striking difference on the Na^+ concentrations necessary to reach saturation, *i.e.*, 1 or 100 mM for the mitochondrial and plasma membrane transporters, respectively. Furthermore the mitochondrial, unlike the plasma membrane, transporter was fully active also in the absence of added Ca^{++} and/or Mg^{++}.

Taken together, the results presented in this study indicate that the U937 cell mitochondrial transporter of AA, because of its very low requirement for Na^+ and independence for Ca^{++} and Mg^{++}, displays kinetic characteristics surprisingly similar with those of the plasma membrane SVCT2.

Keywords: Ascorbic acid transport; Mitochondria; Ascorbic acid; Na^+-dependent ascorbic acid transporter 2

1. Introduction

Vitamin C is a very important water soluble vitamin taken up directly by the cells as L-ascorbic acid (AA) *via* high affinity/low capacity Na^+-dependent transporters 1 and 2 (SVCT1 and 2) [1-3]. In alternative, cells may also take up the vitamin as dehydroascorbic acid (DHA) through hexose transporters [4-5], an event followed by the rapid intracellular reduction back to AA [6-8]. While this second mechanism might appear advantageous because of its high capacity, its involvement is clearly conditioned by the extracellular levels of DHA, normally in the very low micromolar range with some variation associated with the release of AA oxidizing species, as the superoxide anion [9].

Regardless of the mechanism of uptake, however, cells may accumulate large amounts of vitamin C in the cytosol and, at least in principle, in other subcellular compartments provided of adequate transport systems of the vitamin. One of such compartments is represented by the mitochondria, as these organelles actively produce reactive oxygen species and are therefore expected to benefit of the antioxidant activity of AA [10], based on direct scavenging of reactive species [11] and on other activities related to vitamin E recycling [12]. Not surprisingly, mitochondrial vitamin C has been detected in *in vivo* studies and was found to increase upon dietary supplementation of the vitamin [13-15].

The mechanism whereby the vitamin is taken up by the mitochondria has been attributed for a long time to DHA transport for at least two separate reasons: i) hexose transporters are expressed in mitochondria [15-18], despite the lack of an apparent role of glucose in mitochondrial metabolism; ii) a high capacity transport is expected to be advantageous under conditions of extensive mitochondrial formation of reactive oxygen species.

Along the same lines, the possibility of a mitochondrial AA transport has been considered unlikely because of the high affinity of SVCTs, allowing the full expression of their activity at AA concentrations remarkably lower than those detected in the cytosol of many cell types *in vivo* [19-20]. While this consideration deserves further discussion, there are two additional reasons arguing against a role of SVCTs in mitochondrial AA transport. The first one is based on the well established Na^+-dependence of these transporters [1], the activity of which does not appear compatible with the concentrations of the cation in the intracellular fluids. The second reason against the mitochondrial location (and function) of SVCT2 is based on its Ca^{++}-requirements for the expression of maximal activity [21]. Under resting conditions, there is an about four order of magnitude difference in Ca^{++} concentrations between the extra and intracellular compartments, with a possibility of a transient increase upon stimulation [22], however leading to Ca^{++} concentrations still remarkably lower than those found in the extracellular milieu.

The above considerations have therefore stimulated various investigations providing experimental evidence of efficient mitochondrial transport of DHA, however often using high DHA concentrations [15-18]. The available evidence is in any case in keeping with the possibility of a physio-pathological relevance of mitochondrial DHA uptake in some conditions. This mechanism has the advantage of linking DHA formation (and hence the formation of AA oxidizing species) with rapid DHA transport and reduction back to AA. In other words, AA might be rapidly accumulated in mitochondria under the same conditions in which these organelles produce the superoxide anion.

Despite these observations and logical considerations, however, we recently provided evidence for the presence of SVTC2 immunoreactivity in U937 cell mitochondria [23]. Exposure of these cells to AA was associated with the mitochondrial accumulation of even low concentrations of the vitamin. Our results were recently confirmed by another group in a different cell type [24]. These Authors, while providing solid and definitive evidence for the mitochondrial expression of a functional SVCT2, also demonstrated that because of the intracellular environment low in Na^+ and high in K^+, the mitochondrial SVCT2 functions with low affinity.

The present study, confirms and extends our previous findings [23] by showing that the U937 cell mitochondrial AA transporter is surprisingly characterised by a Km similar to that of the plasma membrane SVCT2. An additional similarity was found in the pH-dependence and positive cooperativity for Na^+ ($n_H \cong 2$). Strikingly, however, 100 fold less Na^+ was necessary to maximally support AA transport in mitochondria in comparison with the transport through the plasma membrane. A final critical difference was found for the Ca^{++}/Mg^{++} dependence, as plasma membrane SVCT2 required very high (millimolar) concentrations (normally present in extracellular fluids), in contrast with the mitochondrial transporter, fully active also in the absence of added Ca^{++}. Our results are therefore consistent with the possibility that mitochondrial SVCT2 might function with different affinities, including the very high affinity that the same transporter displays in the plasma membrane. In order to acquire this phenotype, the mitochondrial SVCT2 reduces its cation requirements for optimal activity.

2. Materials and methods

2.1 Chemicals

AA, dithiothreitol (DTT), choline-chloride, 4-Morpholineethanesulfonic acid hemisodium salt (MES) and most of the reagent-grade chemicals were purchased from Sigma-Aldrich (Milan, Italy). Perkin–Elmer Life and Analytical Sciences (Boston, MA, USA) supplied the L-[1-^{14}C]-ascorbic acid (specific activity 5.35 mCi/mmol), which was dissolved in deionized water containing 0.1 mM acetic acid and stored in multiple aliquots at −20°C until use [25]. The antibodies against SVCT2 (sc-9926), cytochrome c (sc-7159) calnexin (sc-6465), HSP-60 (sc-13115), as well as the horseradish peroxidase-conjugated secondary antibodies (sc-2350; sc-2005) were purchased from Santa Cruz Biotechnology (Santa Cruz, CA); antibodies against GLUT3 (ab53095) and lamin A (ANT0072) were from Abcam (Cambridge, UK) and Diatheva (Fano, Italy), respectively.

2.2. Cell culture and treatment conditions

U937 human myeloid leukemia cells and Raw 264.7 murine macrophages were cultured in RPMI 1640 medium (Sigma-Aldrich) supplemented with 10% heat-inactivated FBS (Euroclone, Celbio Biotecnologie, Milan, Italy), penicillin (100 units/ml) and streptomycin (100 µg/ml) (Euroclone). The cells were grown at 37°C in T-75 tissue culture flasks (Corning, Corning, NY) gassed with an atmosphere of 95% air-5% CO_2. Cells (1×10^6 cells/ml) were exposed for 5 min to AA or ^{14}C-AA (specific activity 5.35 mCi/mmol) in Extracellular Buffer, EB (15 mM Hepes, 135 mM NaCl, 5 mM KCl, 1.8 mM $CaCl_2$, 0.8 mM $MgCl_2$, pH 7.4) in the presence of 0.1 mM DTT.
A 10 mM AA stock solution was prepared in immediately before use.
Stability of AA (30 µM) in the above EB was assessed by monitoring the absorbance at 267 nm for 90 min (ε_{267}=14,600 M^{-1} cm^{-1}). In selected experiments, NaCl was replaced with choline-chloride.

2.3. Measurement of ascorbic acid content by HPLC

After treatments, the cells or mitochondria were washed twice with cold EB or IB respectively and the final pellets were extracted with ice-cold 70% (v/v) methanol/30% solution (10 mM tetrabutylammonium hydrogen sulfate, 10 mM KH_2PO_4, 0.5% methanol, pH 6.0) containing 1 mM EDTA and 10 mM DTT. After 10 min at ice bath temperature, the samples were centrifuged at 10,000*g* for 20 min at 4 °C. Samples were filtered through a 0.22 µm filter (Millipore Corporation, Billerica, MA, USA) and either analyzed immediately or frozen at −80 °C for later analysis. AA content was measured by HPLC with the UV detection wavelength set at 265 nm, as described in [26], with minor modifications. The assay involved the use of a 15 cm × 4.6 mm Discovery C-18, 5 µm column (Supelco, Bellefonte, PA, USA) equipped with a Supelguard Discovery C-18 guard column (2 cm × 4 mm, 5 µm). The injection volume was 20 µl. Under these conditions the retention

time of AA was about 4 min. AA concentration was determined from the corresponding calibration curve constructed with the pure chemical AA dissolved in the extraction solution.

2.4. Measurement of ^{14}C-AA cellular uptake

Uptake was stopped by washing the cells two times with ice-cold EB, containing an excess of unlabeled AA. Cells were then dissolved in 0.5 M NaOH and the incorporated radioactivity was measured by liquid scintillation spectrometry. The ^{14}C-AA non-specific binding to cells was assayed by performing the experiments at 0 °C. No differences between the controls (untreated samples) and 0 °C-^{14}C-AA-treated samples were detected.

2.5 Mitochondria isolation and subcellular fractionation

Mitochondria (M) were isolated either by differential centrifugation, as detailed in [27] or by sucrose density gradient centrifugation, as described by Koziel et al., [28] with minor modifications. The latter method was also used to obtain the other sub-cellular fractions: nucleus (N), plasma membranes (PM), endoplasmic reticulum (ER) and cytosol (C). Briefly, cells were washed twice in PBS and resuspended in cold homogenization buffer (HB: 225 mM mannitol, 75 mM sucrose, 0.1 mM EGTA, 5 mM Tris-HCl, pH 7.4), in presence of protease inhibitor cocktail and digitonin (10 µg/ml) and homogenized using a glass potter in an ice-bath. The efficiency of homogenization was monitored under the microscope using trypan blue and stopped when the 90% of the total cells was disintegrated. The homogenate was centrifuged at 1000x*g* for 10 min at 4°C and the supernatant (S1) was collected for the final centrifugation. The pellet was re-homogenized and the supernatant (S2) added to S1 and centrifuged at 20000x*g* for 20 min at 4°C. The pellet obtained, containing nucleus fraction (**N**), was maintained at -20°C till use. The supernatant was centrifuged at 100000x*g* for 60 min at 4 °C to obtain the endoplasmic reticulum fraction (**ER**, pellet) and the cytosol (**C,** supernatant). The pellet obtained from the centrifugation of S1+S2 was resuspended in 5 mM MES, 0.2 mM EDTA pH 6.0 and separated by centrifugation at 20000x*g* for 2 hours at 4 °C on a discontinuous 38%, 43% and 53% sucrose gradient. The middle density band corresponding to mitochondrial fraction (**M**) and the high density band corresponding to the plasma membranes (**PM**) were collected and centrifuged two times in HB at 20000x*g* for 20 min.

2.6. Incubation of U937 cell mitochondria with ^{14}C-AA

Isolated mitochondria were exposed for 3 min to ^{14}C-AA in Mitochondrial Buffer, MB (5 mM HEPES, 210 mM mannitol, 70 mM sucrose, 1 mM Na-EGTA, pH 7.4) or Intracellular Buffer, IB (15 mM HEPES-Na, 15 mM NaCl, 120 mM KCl, 1 mM $MgCl_2$, pH 7.6) and processed as

described below. For experiments in Na^+-free MB, Na-EGTA was replaced with choline-chloride in EGTA Na^+-free, while for experiments in Na^+-free IB, HEPES-Na^+ and NaCl was replaced with choline-chloride in HEPES Na^+-free.

MB without EGTA was used in experiments aimed at evaluating the role of cations in AA transport. Uptake was stopped by rinsing the mitochondria with ice-cold MB or IB, containing an excess of unlabeled AA. Mitochondrial pellets were then dissolved in 0.5 M NaOH and the incorporated radioactivity was measured by liquid scintillation spectrometry. The ^{14}C-AA non-specific binding to mitochondria was assayed by performing the experiments at 0 °C. No differences between the controls (untreated samples) and 0 °C-^{14}C-AA-treated samples were detected.

2.7 Immunolocalization by confocal microscopy

U937 cells were incubated for 20 min with 50 nM MitoTraker Red CMXRos (Molecular Probes, Europe, Leiden, The Netherlands) in 2 ml of saline A (8.182 g/L NaCl, 0.372 g/L KCl, 0.336 g/L $NaHCO_3$, and 0.9 g/L glucose, pH 7.4) in 35 mm glass bottom culture dishes (MatTek, Ashland, MA). The cells were then fixed for 1 min with 95% ethanol/5% acetic acid, washed with PBS (8 g/l NaCl, 1.15 g/l Na_2HPO_4, 0.2 g/l KH_2PO_4, and 0.2 g/l KCl, pH 7.4) and blocked in PBS containing 2% w/v bovine serum albumin (BSA) for 30 min at room temperature. The cells were subsequently incubated with goat polyclonal anti-SVCT2 antibody (1:100 in PBS containing 2% BSA), stored for 18 h at 4°C, washed and then exposed to FITC-conjugated secondary antibody diluted 1/100 in PBS for 2 h in the dark. The digital images were acquired on a Leica TCS-SP5 CSLM mounted on a Leica DMI 6000 CS inverted microscope (Leica Microsystems CMS GmbH, Mannheim, Germany) at 1024x1024 using 63.0 x 1.4 oil objective (HCX PL APO 63.0 x 1.40 OIL UV) and with appropriate excitation / detection settings (FITC argon laser 488 nm / 500-535 nm emission filter; MitoTracker Red HeNe laser 543 nm / 555-610 nm emission filter). Images and degree of co-localization were analyzed by the Leica Application Suite Advanced Fluorescence (LASAF) and ImageJ Software (Wayne Rasband, Bethesda, MA). Semi-quantitative analysis with the JACoPImageJ tool provided Pearson's (PC) and Manders' (M1 and 2) overlaps coefficients (http://rsb.info.nih.gov/ij/plugins/track/jacop.html). The co-localization of SVCT2 (green) with mitochondria (red) is shown as yellow (merged). M1 indicates the overlap coefficient of SVCT2 to mitochondria, while M2 signifies the correlation of mitochondria overlapping SVCT2. The Pearson's and Manders' overlap coefficients are represented as the average of ten individual cells.

2.8 Western blot assay

Equal amount (30 μg) of sub-cellular fractions and whole cell lysates were resolved in 12.5 or 15% sodium dodecyl sulphate polyacrylamide gel and electrotransferred to polyvinyldiene difluoride membranes. Western blot analyses were performed using antibodies against SVCT2, cytochrome c, calnexin, HSP-60, GLUT3 and lamin A. Details on Western blotting apparatus and conditions are reported elsewhere [29]. Antibodies against cytochrome c, calnexin, GLUT3 and lamin A were used to assess the purity of the fractions; the antibody against HSP-60 was used to assess the equal loading of the lanes.

2.9. Kinetic calculations

The transport kinetic parameters were calculated by using the Michaelis-Menten equation and the linear transformation of Eadie-Hofstee. Kinetic parameters were estimated from the fitted curves using the Graph Pad Prism software designed for nonlinear regression analysis.

3. Results

3.1. Mitochondrial localization of anti-SVCT2 immunoreactivity

We performed immunocytochemical analysis of U937 cells labelled with anti-SVCT2 antibodies and with a mitochondrial probe, MitoTracker red CMXRos. Figure 1 (A-D) provides the image of a single cell, however representative of the remaining cells, in which the green identifies the expression of SVCT2 (A), the red the mitochondria (B) and the yellow the colocalized pixels in the overlay image (C). Co-localization analysis and quantification were also performed using Image J software, where background and threshold were set, generating a co-localization image (co-localised pixels in white) (D). Panel E shows the Pearson's and Manders' overlap coefficients derived with the JACoPImageJ tool. The calculated Pearson's coefficient (PC) was 0.77 and Manders' coefficient M1 indicates that 93,2% of the SVCT2 detected overlaps with CMXRos-stained mitochondria, thereby further emphasising the existence of a very high level of co-localization of the two fluorophores. Immunoblotting experiments using mitochondria isolated by differential centrifugation as well as by sucrose gradient centrifugation provided results coherent with the above findings (Figure 1F). We next used an additional method for subcellular fractionation to obtain nuclear, mitochondrial, plasma membrane, endoplasmic reticulum and cytosol enriched fractions. As indicated in Figure 1G, SVCT2 expression was restricted to the mitochondrial and plasma membranes, in which expression of their respective markers, *i.e.*, cytochrome c for the mitochondria [23] and GLUT 3 for the plasma membrane (note that there was no GLUT 3 expression in the mitochondrial fraction, as reported by other authors, [30-31] was also detected. A weak SVCT2 expression, probably associated with mitochondrial and plasma membrane contaminations, was found in the nuclear fraction (expressing lamin A) [32]. Lamin A expression was however absent in mitochondria and plasma membranes. An additional consideration is on the expression of calnexin, a marker of the endoplasmic reticulum [24], also detected in the plasma membrane fraction and, as a very weak band, in the mitochondrial fraction. It is however unlikely that such a contamination (endoplasmic reticulum) provides the anti-SVCT2 reactivity to the plasma membrane or mitochondrial fraction since no anti-SVCT2 reactivity was found in the endoplasmic reticulum enriched fraction. There was no SVCT2 immunoreactivity in the cytosol.

Collectively, these results are in keeping with the notion that anti-SVCT2 antibodies recognise a protein(s) in mitochondria, as we previously reported [23].

3.2. Kinetic properties of the mitochondrial transporter of AA

We examined the kinetic properties of the AA transporter in mitochondria isolated from U937 cells. Time course analysis of AA uptake, performed in MB at a 30 μM substrate concentration, revealed that mitochondria take up AA at a constant rate of 0.48 ± 0.055 nmol/mg prot/min for at least 5 min (Figure 2A). We next performed experiments using mitochondria exposed for 3 min to increasing concentrations of AA and obtained a response described by a hyperbolic curve saturating at 60 μM AA (Figure 2B). Analysis of the transport data by the Eadie-Hofstee method (Figure 2C) produced a straight line (r^2=0.95), consistent with the presence of a single functional component, allowing the calculation of an apparent Km of 26.96 ± 1.46 μM and a Vmax of 1.24 ± 0.045 nmol/mg prot/min (n=5). Experiments were next performed using IB and AA concentrations up to 1.5 mM, as previous studies from Muñoz-Montesino [24] identified a sigmoidal concentration response curve under similar conditions. A 3 min incubation was also used in these experiments, a condition allowing the assessment of kinetic parameters under initial velocity conditions also after exposure to these high AA concentrations (not shown). Results illustrated in Figure 2D, however, are in keeping with those obtained with MB and analysis by the Eadie-Hofstee method (Figure 2E) revealed an apparent Km value of 22.4 ± 1.6 μM and a Vmax of 0.91 ± 0.036 nmol/mg prot/min. The last set of experiments analysed the pH sensitivity of the mitochondrial AA transporter. Results illustrated in Figure 2F provide evidence for a progressive loss of activity at descending pH values.

We also performed experiments using intact Raw 264.7 cells, which exclusively express SVCT2 (Figure 3A, inset a). These cells were first exposed for 5 min to increasing concentrations of AA and then processed for the assessment of AA content. The concentration-dependent accumulation of the vitamin is reported in the inset (b) to Figure 3A. Eadie-Hofstee analysis of these data (Figure 3A) produced a straight line (r^2=0.95), as previously shown for U937 cell mitochondria (Figures 2C and E), allowing the calculation of a similar Km value (22.4 ± 1.7 μM). To draw a comparison, similar experiments were performed in U937 cells, which express both SVCT1 and 2 (Figure 3B, inset a). These experiments generated a hyperbolic dose-response curve (Figure 3B, inset b) that, when analysed by the Eadie-Hofstee method (Figure 3B), revealed a non-linear relationship that fits well with a model describing the involvement of two saturable transport systems for AA, each with different affinities for the substrate. The higher affinity component had an apparent transport Km of 8.4 ± 0.76 μM and Vmax of 0.11 ± 0.007 nmol/mg prot/min, whereas the lower affinity component had apparent Km and Vmax values of 85.5 ± 7.9 μM and 0.48 ± 0.03 nmol/mg prot/min, respectively. These Km values fall within the expected range for SVTC2 and for SVCT1 [2, 33-35]. We finally determined in intact Raw 264.7 cells the pH effect of plasma membrane SVCT2-dependent AA transport. Under these conditions the sensitivity to extracellular pH (Figure 3C) was remarkably similar to that previously described by other authors [36-37]. It is interesting to note that

the pH sensitivity of mitochondrial SVCT2-dependent transport of AA illustrated in Figure 2F is also identical to the one described for plasma membrane (Figure 3C), in keeping with the notion that the activity of mitochondrial SVCT2 is impaired at acid pH, as previously observed in intact cells [36-37].

Taken together, the above results indicate that AA transport Km values of mitochondrial and plasma membrane SVCT2 are remarkably similar.

3.3. Na^+-dependence of mitochondrial SVCT2

Plasma membrane SVCT2-mediated transport of AA is activated by high Na^+ concentrations, *i.e.*, those normally detected in the extracellular milieu [21]. The Na^+-dependence of AA transport was therefore investigated in mitochondria isolated from U937 cells. The results illustrated in Figure 4A are from experiments in which MB was supplemented with 30 μM AA and increasing concentrations of Na^+. These results clearly establish the Na^+-dependent activation of the mitochondrial SVCT2 at surprisingly low concentrations of the cation. Indeed, mitochondrial uptake of AA increased linearly with increasing Na^+ concentrations, reaching a plateau at 1 mM, with a Na_{50} (the Na^+ concentration inducing a 50% of the AA maximal uptake rate) of 0.525 mM. We then performed similar experiments in which MB was replaced with IB. As indicated in Figure 4B, AA uptake was somewhat increased under these conditions but, most importantly, the plateau was reached once again at 1 mM Na^+. The sigmoidal curves outlined in Figures 4A and B are indicative of a cooperative mechanism, also emphasised by the Hill plot (insets to Figures 4A and B) leading to a calculated n_H values of 2.2 ± 0.1 and 2.0 ± 0.16, respectively.

We finally tested the Na^+-dependence for AA transport in Raw 264.7 cells and obtained data in line with those previously reported in other studies [21]. In particular, AA transport rate reached a plateau at Na^+ concentrations above 100 mM (Figure 4C), with a remarkably lower transport rate of the vitamin observed at 15 mM Na^+, *i.e.* the cytosolic concentration of the cation. Under these conditions, the Hill plot (Figure 4C, inset) led to a calculated n_H values of 2.05 ± 0.19.

Taken together, these results show that AA transport is Na^+-dependent in the case of both the plasma membrane and mitochondrial SVCT2. In addition, an identical Na^+ cooperativity was detected despite the remarkably different levels of the cation necessary to maximally activate AA transport in mitochondria or plasma membrane.

3.4. Ca^{++}- and Mg^{++}- dependence of mitochondrial SVCT2

Plasma membrane SVCT2-mediated transport of AA has an absolute requirement for Ca^{++} and Mg^{++} [21]. Coherently, omission of these cations from the extracellular milieu abolished AA

(30 μM) transport in Raw 264.7 cells, whereas hardly any effect was obtained with omission of either Ca^{++} or Mg^{++} alone (Figure 5A). Results obtained in U937 cells were somewhat different, as some residual AA transport activity was found in the absence of both cations (Figure 5A), most likely dependent on SVCT1 activity.

These results are therefore different from those reported in Figure 2B (using isolated mitochondria), in which AA transport studies were performed using a Ca^{++}/Mg^{++}-free buffer supplemented with EGTA (MB). Further studies revealed that AA (30 μM) transport in isolated mitochondria is not affected by removal of EGTA and is abolished by Na^{+} omission, regardless of the presence of EGTA. Moreover, AA transport rate in EGTA-free MB was insensitive to addition of Ca^{++} (0.25 μM) and/or Mg^{++} (2.5 mM) (Figure 5B). The Ca^{++} and/or Mg^{++} independence of AA transport in isolated mitochondria was also established in experiments in which MB was replaced with IB (not shown).

These results therefore indicate that mitochondrial SVCT2-dependent AA transport is Ca^{++} and Mg^{++}-independent and is not further stimulated by increases in Ca^{++} and/or Mg^{++} concentrations.

4. Discussion

There is a growing interest on the effects of vitamin C in various subcellular compartments and a need to understand the specific relevance of the transport mechanisms involved in its accumulation in these specific sites. Mitochondria represent an important example, as vitamin C is expected to play an array of critical functions in these organelles in which, for the reasons summarised in the Introduction section, DHA uptake has been considered of pivotal importance for vitamin supply [15-18]. Based on these considerations, we were initially surprised to detect anti-SVCT2 immunoreactivity in the mitochondria isolated from U937 cells [23]. The present work implements these observations with the direct detection of a punctuate fluorescence response elicited by the anti-SVCT2 antibodies, largely colocalizing with the fluorescence elicited by a mitochondrial probe (Figure 1A-E), and with the identification of the same bands in immunoblot experiments using anti-SVCT2 antibodies and mitochondrial preparations, obtained with two different isolation procedures (Figure 1F). The mitochondrial localization of SVCT2 is also consistent with the results obtained in immunoblotting experiments using markers for the nuclear, mitochondrial, plasma membrane, endoplasmic reticulum and cytosol enriched fractions (Figure 1 G). These results are therefore in line with the findings of the elegant and comprehensive work of Muñoz-Montesino et al [24], that provided solid scientific ground to support our initial observation on the mitochondrial SVCT2 [23].

The most important finding obtained in this study is however on the affinity of the mitochondrial AA transporter, which would be expected to be low if the requirements for optimal activity were the same as those of the plasma membrane transporter [21]. This prediction, however, was not confirmed by the results of our kinetic studies, providing evidence for a mitochondrial transport of AA, saturating at 5 min (Figure 2A), characterised by a dose-response curve (Figure 2B) which, analysed by the Eadie-Hofstee method (Figure 2C), leads to a Km of 26.96 ± 1.46 μM. It is interesting to note that similar experiments using a K^+-containing buffer produced identical results (Figure 2D and E) with an even lower Km (22.40 ± 1.6 μM), despite the recent indication that K^+ may in fact reduce the affinity of the mitochondrial AA transporter [24]. Km values calculated in our studies are remarkably similar to those reported by other authors for plasma membrane transport in various cell types [2, 21, 38-39]. We also report a Km of 22.4 ± 1.66 μM for AA uptake in Raw 264.7 cells (Figure 3A), which only express SVCT2 (Figure 3A, inset a). In U937 cells, which express both SVCT1 and 2 (Figure 3B, inset a), the SVCT2 Km value obtained, 8.4 ± 0.76 μM (Figure 3B), is similar to SVCT2 Km values in cellular systems expressing both transporters [2, 33-35]. An additional important similarity was found for the pH-dependent

regulation of SVCT2-mediated AA transport. Our results obtained with intact Raw 264.7 cells (Figure 3C) are in keeping with the notion that SVCT2 activity is impaired at acid pH [36-37] and a virtually superimposable curve was obtained in experiments performed with isolated mitochondria (Fig. 2F).

In summary, our results provide evidence for remarkable similarities between the mitochondrial AA transporter and the plasma membrane SVCT2, including the very low Km values. As in the case of the plasma membrane SVCT2, the mitochondrial AA transporter was also found to interact with Na^+ in a cooperative manner, but required 100 times less Na^+ for maximal activity (Figure 4A and B). This observation is compatible with, and provides an explanation for, the unexpected high affinity of a transporter expressing maximal activity in an intracellular environment, characterised by concentrations of Na^+ largely lower that those necessary to maximally drive AA transport through the plasma membrane (Figure 4C). It should be also noted that the use of a low (Figure 4A) *vs* high (Figure 4B) K^+ medium produces hardly any effect on the Na^+-dependent regulation of mitochondrial AA transport. Additional important information, also coherent with the expression of the maximal activity in an intracellular environment, is that i) the mitochondrial AA transporter was fully active also in the absence of Ca^{++} and Mg^{++} and that ii) transport activity was not affected by the addition of each, or both, of these cations (Figure 5).

The above results are of complex interpretation. For example, it appears very difficult to find a reasonable explanation for the need of only 1 mM Na^+ to maximally support mitochondrial transport of AA, whereas a 10-fold difference in the extra *vs* intracellular Na^+ concentrations is instead necessary to achieve the same result for the plasma membrane SVCT2. It is important to note that our experiments were performed in isolated mitochondria and that we do not know the exact intramitochondrial concentration of Na^+ after the isolation procedure of these organelles. We can however predict that, as normally observed in intact cells [40], the ratio is maintained close to 1, which then raises concerns for the formation of the electrochemical gradient necessary for AA transport. Clearly, more studies are necessary to provide an answer to such an intriguing question and to find an explanation for the K^+-independence of the low Km transporter (Figure 2B and D) *vs* the reported inhibitory response mediated by K^+ on the low Km transporter [24]. The possible answer for the different cation dependence is likely based on the different compositions of the inner mitochondrial membrane *vs* plasma membrane, which may favour interactions with specific components and result in different structural organization.

An additional important question to be asked is why cells should use a low Km active transport for mitochondrial AA uptake *in vivo*. Most cell types indeed contain large amounts of the vitamin in their cytosol [2,3,10]. The question, rephrased, would then be why should cells use a

mitochondrial transporter always working at saturating substrate concentrations? Does it make sense? The obvious answer is clearly that high affinity transport is relevant when the substrate concentration is low but nevertheless this phenomenon is not unique. For example, we should keep in mind that SVCT2 is largely expressed in the plasma membrane of neurons bathed in a milieu containing 200/400 μM AA [41]. The substrate saturation phenomenon is therefore observed in different contexts and hence appears of plausible physiological significance. We therefore believe that the apparent dichotomy existing between the low Km of the transporter and the high substrate concentration could be justified by the existence of mechanisms regulating transporter activity (in specific cell types or in the mitochondria of specific cells types) by direct inhibition, as we recently described with DHA [42]. Exogenous molecules, as quercetin of phloretin [43], or the activation of specific signal transduction pathways [44], may also regulate AA transporter activity.

Our results are therefore unexpected, but nevertheless appear of likely physiological significance, at least for some cell types. For other cell types there is the more straightforward possibility, proposed by Godoy et al [21], that SVCT2 exists in two different functional states defined by their respective subcellular localization. Which, reinterpreted, means that the mitochondrial AA transporter should display a low affinity since the conditions are not permissive for the expression of optimal activity. In a recent study [24], the same group reported that this transport activity is indeed characterised by a low affinity. In this perspective mitochondrial transport of the vitamin appears regulated by the low affinity of the transporter.

We have two additional considerations on our findings. The first one is that the discovery of functional SVCT2 expression in mitochondria will most likely foster the research on the biological and physiopathological relevance [45] of AA subcellular compartmentalization and on the mechanisms regulating these events. In this context, the same heterogenicity observed for plasma membrane SVCT2 in different cell types and conditions is to be expected also for the mitochondrial form of the transporter. At least in principle, different cell types could meet their requirements for mitochondrial AA accumulation with the use of high or low affinity transporters, or none of them, thereby limiting the access to the oxidized form of the vitamin. Clearly, much more work is needed to determine whether the above possibilities are indeed correct or are in fact confuted by the experimental evidence.

The second consideration is still based on the concept of heterogenicity. The existence of low affinity transport in cultured cells detected in the work by Muñoz-Montesino et al. [24] rules out the possibility that the high affinity transport detected in our cells arises as a consequence of a cell culture effect associated with the growth of the cells in AA-free medium. Coherently,

experiments in progress in our laboratory demonstrate the presence of a low affinity transport of AA in the mitochondria derived from Raw 264.7 cells (not shown) grown in the same medium in which the U937 cells are also grown.

The mitochondrial localization of vitamin C has thus far received very little attention, although there are reasons to predict important effects in an array of mitochondrial events. In this perspective, the mechanisms whereby vitamin C is taken up by these organelles appears of pivotal importance. For example, we recently found that sequential activities of high affinity transporters of AA in the plasma membrane and mitochondria effectively prevent apoptosis mediated by arsenite, a toxic compounds directly targeting mitochondria [46]. In addition, cytoprotection is observed after exposure to extremely low concentrations of the vitamin and appears exclusively associated with its mitochondrial fraction.

In conclusion, our work provides further evidence for the mitochondrial localization of SVCT2 in U937 cells and demonstrates that this transporter, because of the very low requirements for Na^+ and divalent cations, has an affinity comparable with that of the plasma membrane SVCT2. While future studies should address the generality and molecular bases of this phenomenon, these results nevertheless imply that different cell types might accumulate vitamin C in their mitochondria through both high and low affinity SVCT2.

Funding sources

This work was supported by Ministero dell'Università e della Ricerca Scientifica e Tecnologica, Programmi di Ricerca Scientifica di Rilevante Interesse Nazionale, 2010-2011, (Grant number: 20108YB5W3-001, O.C.).

Conflict of interest

The authors declare no conflict of interest

References

[1] H. Tsukaguchi, T. Tokui, B. Mackenzie, U.V. Berger, X.Z. Chen, Y. Wang, R.F. Brubaker, M.A. Hediger, A family of mammalian Na+-dependent L-ascorbic acid transporters, Nature, 399 (1999) 70-75.

[2] I. Savini, A. Rossi, C. Pierro, L. Avigliano, M.V. Catani, SVCT1 and SVCT2: key proteins for vitamin C uptake, Amino Acids, 34 (2008) 347-355.

[3] H. Takanaga, B. Mackenzie, M.A. Hediger, Sodium-dependent ascorbic acid transporter family SLC23, Pflugers Arch, 447 (2004) 677-682.

[4] J.C. Vera, C.I. Rivas, J. Fischbarg, D.W. Golde, Mammalian facilitative hexose transporters mediate the transport of dehydroascorbic acid, Nature, 364 (1993) 79-82.

[5] S.C. Rumsey, O. Kwon, G.W. Xu, C.F. Burant, I. Simpson, M. Levine, Glucose transporter isoforms GLUT1 and GLUT3 transport dehydroascorbic acid, J Biol Chem, 272 (1997) 18982-18989.

[6] W.W. Wells, D.P. Xu, Y.F. Yang, P.A. Rocque, Mammalian thioltransferase (glutaredoxin) and protein disulfide isomerase have dehydroascorbate reductase activity, J Biol Chem, 265 (1990) 15361-15364.

[7] B.S. Winkler, S.M. Orselli, T.S. Rex, The redox couple between glutathione and ascorbic acid: a chemical and physiological perspective, Free Radic Biol Med, 17 (1994) 333-349.

[8] J.M. May, S. Mendiratta, K.E. Hill, R.F. Burk, Reduction of dehydroascorbate to ascorbate by the selenoenzyme thioredoxin reductase, J Biol Chem, 272 (1997) 22607-22610.

[9] M. Fiorani, C. Azzolini, L. Cerioni, A. Guidarelli, O. Cantoni, Superoxide dictates the mode of U937 cell ascorbic acid uptake and prevents the enhancing effects of the vitamin to otherwise nontoxic levels of reactive oxygen/nitrogen species, J Nutr Biochem, 24 (2013) 467-474.

[10] S.J. Padayatty, A. Katz, Y. Wang, P. Eck, O. Kwon, J.H. Lee, S. Chen, C. Corpe, A. Dutta, S.K. Dutta, M. Levine, Vitamin C as an antioxidant: evaluation of its role in disease prevention, J Am Coll Nutr, 22 (2003) 18-35.

[11] S. Singh, S.V. Rana, Ascorbic acid improves mitochondrial function in liver of arsenic-treated rat, Toxicol Ind Health, 26 (2010) 265-272.

[12] M.G. Traber, J.F. Stevens, Vitamins C and E: beneficial effects from a mechanistic perspective, Free Radic Biol Med, 51 (2011) 1000-1013.

[13] K. Ramanathan, S. Shila, S. Kumaran, C. Panneerselvam, Ascorbic acid and alpha-tocopherol as potent modulators on arsenic induced toxicity in mitochondria, J Nutr Biochem, 14 (2003) 416-420.

[14] O.C. Ingebretsen, P.T. Normann, Transport of ascorbate into guinea pig liver mitochondria, Biochim Biophys Acta, 684 (1982) 21-26.

[15] X. Li, C.E. Cobb, K.E. Hill, R.F. Burk, J.M. May, Mitochondrial uptake and recycling of ascorbic acid, Arch Biochem Biophys, 387 (2001) 143-153.

[16] S. KC, J.M. Carcamo, D.W. Golde, Vitamin C enters mitochondria via facilitative glucose transporter 1 (Glut1) and confers mitochondrial protection against oxidative injury, FASEB J, 19 (2005) 1657-1667.

[17] X. Li, C.E. Cobb, J.M. May, Mitochondrial recycling of ascorbic acid from dehydroascorbic acid: dependence on the electron transport chain, Arch Biochem Biophys, 403 (2002) 103-110.

[18] Y.C. Lee, H.Y. Huang, C.J. Chang, C.H. Cheng, Y.T. Chen, Mitochondrial GLUT10 facilitates dehydroascorbic acid import and protects cells against oxidative stress: mechanistic insight into arterial tortuosity syndrome, Hum Mol Genet, 19 (2010) 3721-3733.

[19] A.C. Carr, S.M. Bozonet, J.M. Pullar, J.W. Simcock, M.C. Vissers, Human skeletal muscle ascorbate is highly responsive to changes in vitamin C intake and plasma concentrations, Am J Clin Nutr, 97 (2013) 800-807.

[20] M. Levine, S.J. Padayatty, M.G. Espey, Vitamin C: a concentration-function approach yields pharmacology and therapeutic discoveries, Adv Nutr, 2 (2011) 78-88.

[21] A. Godoy, V. Ormazabal, G. Moraga-Cid, F.A. Zuniga, P. Sotomayor, V. Barra, O. Vasquez, V. Montecinos, L. Mardones, C. Guzman, M. Villagran, L.G. Aguayo, S.A. Onate, A.M. Reyes, J.G. Carcamo, C.I. Rivas, J.C. Vera, Mechanistic insights and functional determinants of the transport cycle of the ascorbic acid transporter SVCT2. Activation by sodium and absolute dependence on bivalent cations, J Biol Chem, 282 (2007) 615-624.

[22] R.J. Kaufman, J.D. Malhotra, Calcium trafficking integrates endoplasmic reticulum function with mitochondrial bioenergetics, Biochim Biophys Acta, (2014).

[23] C. Azzolini, M. Fiorani, L. Cerioni, A. Guidarelli, O. Cantoni, Sodium-dependent transport of ascorbic acid in U937 cell mitochondria, IUBMB Life, 65 (2013) 149-153.

[24] C. Munoz-Montesino, F.J. Roa, E. Pena, M. Gonzalez, K. Sotomayor, E. Inostroza, C.A. Munoz, I. Gonzalez, M. Maldonado, C. Soliz, A.M. Reyes, J.C. Vera, C.I. Rivas, Mitochondrial ascorbic acid transport is mediated by a low-affinity form of the sodium-coupled ascorbic acid transporter-2, Free Radic Biol Med, 70 (2014) 241-254.

[25] H. Qiao, J.M. May, Macrophage differentiation increases expression of the ascorbate transporter (SVCT2), Free Radic Biol Med, 46 (2009) 1221-1232.

[26] I. Savini, S. Duflot, L. Avigliano, Dehydroascorbic acid uptake in a human keratinocyte cell line (HaCaT) is glutathione-independent, Biochem J, 345 (2000) 665-672.

[27] M. Fiorani, A. Guidarelli, M. Blasa, C. Azzolini, M. Candiracci, E. Piatti, O. Cantoni, Mitochondria accumulate large amounts of quercetin: prevention of mitochondrial damage and release upon oxidation of the extramitochondrial fraction of the flavonoid, J Nutr Biochem, 21 (2010) 397-404.

[28] K. Koziel, M. Lebiedzinska, G. Szabadkai, M. Onopiuk, W. Brutkowski, K. Wierzbicka, G. Wilczynski, P. Pinton, J. Duszynski, K. Zablocki, M.R. Wieckowski, Plasma membrane associated membranes (PAM) from Jurkat cells contain STIM1 protein is PAM involved in the capacitative calcium entry?, Int J Biochem Cell Biol, 41 (2009) 2440-2449.

[29] O. Cantoni, I. Tommasini, L. Cerioni, The arachidonate-dependent survival signaling preventing toxicity in monocytes/macrophages exposed to peroxynitrite, Methods Enzymol, 441 (2008) 73-82.

[30] P. Cisternas, C. Silva-Alvarez, F. Martinez, E. Fernandez, L. Ferrada, K. Oyarce, K. Salazar, J.P. Bolanos, F. Nualart, The oxidized form of vitamin C, dehydroascorbic acid, regulates neuronal energy metabolism, J Neurochem, 129 (2014) 663-671.

[31] A. Szarka, T. Balogh, In silico aided thoughts on mitochondrial vitamin C transport, J Theor Biol, 365 (2015) 181-189.

[32] K.T. Gagnon, L. Li, B.A. Janowski, D.R. Corey, Analysis of nuclear RNA interference in human cells by subcellular fractionation and Argonaute loading, Nat Protoc, 9 (2014) 2045-2060.

[33] J. Mandl, A. Szarka, G. Banhegyi, Vitamin C: update on physiology and pharmacology, Br J Pharmacol, 157 (2009) 1097-1110.

[34] M. Castro, T. Caprile, A. Astuya, C. Millan, K. Reinicke, J.C. Vera, O. Vasquez, L.G. Aguayo, F. Nualart, High-affinity sodium-vitamin C co-transporters (SVCT) expression in embryonic mouse neurons, J Neurochem, 78 (2001) 815-823.

[35] C.C. Portugal, T.G. da Encarnacao, R. Socodato, S.R. Moreira, D. Brudzewsky, A.F. Ambrosio, R. Paes-de-Carvalho, Nitric oxide modulates sodium vitamin C transporter 2 (SVCT-2) protein expression via protein kinase G (PKG) and nuclear factor-kappaB (NF-kappaB), J Biol Chem, 287 (2012) 3860-3872.

[36] V. Ormazabal, F.A. Zuniga, E. Escobar, C. Aylwin, A. Salas-Burgos, A. Godoy, A.M. Reyes, J.C. Vera, C.I. Rivas, Histidine residues in the Na+-coupled ascorbic acid transporter-2 (SVCT2) are central regulators of SVCT2 function, modulating pH sensitivity, transporter

kinetics, Na+ cooperativity, conformational stability, and subcellular localization, J Biol Chem, 285 (2010) 36471-36485.

[37] S. Luo, Z. Wang, V. Kansara, D. Pal, A.K. Mitra, Activity of a sodium-dependent vitamin C transporter (SVCT) in MDCK-MDR1 cells and mechanism of ascorbate uptake, Int J Pharm, 358 (2008) 168-176.

[38] R. Daruwala, J. Song, W.S. Koh, S.C. Rumsey, M. Levine, Cloning and functional characterization of the human sodium-dependent vitamin C transporters hSVCT1 and hSVCT2, FEBS Lett, 460 (1999) 480-484.

[39] I. Savini, M.V. Catani, G. Duranti, R. Ceci, S. Sabatini, L. Avigliano, Vitamin C homeostasis in skeletal muscle cells, Free Radic Biol Med, 38 (2005) 898-907.

[40] E. Murphy, D.A. Eisner, Regulation of intracellular and mitochondrial sodium in health and disease, Circ Res, 104 (2009) 292-303.

[41] K. Salazar, G. Cerda, F. Martinez, J.M. Sarmiento, C. Gonzalez, F. Rodriguez, M. Garcia-Robles, J.C. Tapia, M. Cifuentes, F. Nualart, SVCT2 transporter expression is post-natally induced in cortical neurons and its function is regulated by its short isoform, J Neurochem, 130 (2014) 693-706.

[42] M. Fiorani, C. Azzolini, A. Guidarelli, L. Cerioni, O. Cantoni, A novel biological role of dehydroascorbic acid: Inhibition of Na(+)-dependent transport of ascorbic acid, Pharmacol Res, 84 (2014) 12-17.

[43] T. Caprile, K. Salazar, A. Astuya, P. Cisternas, C. Silva-Alvarez, H. Montecinos, C. Millan, M. de Los Angeles Garcia, F. Nualart, The Na+-dependent L-ascorbic acid transporter SVCT2 expressed in brainstem cells, neurons, and neuroblastoma cells is inhibited by flavonoids, J Neurochem, 108 (2009) 563-577.

[44] X. Wu, L.H. Zeng, T. Taniguchi, Q.M. Xie, Activation of PKA and phosphorylation of sodium-dependent vitamin C transporter 2 by prostaglandin E2 promote osteoblast-like differentiation in MC3T3-E1 cells, Cell Death Differ, 14 (2007) 1792-1801.

[45] G. Banhegyi, A. Benedetti, E. Margittai, P. Marcolongo, R. Fulceri, C.E. Nemeth, A. Szarka, Subcellular compartmentation of ascorbate and its variation in disease states, Biochim Biophys Acta, 1843 (2014) 1909-1916.

[46] A. Guidarelli, M. Fiorani, C. Azzolini, L. Cerioni, M. Scotti, O. Cantoni, U937 cell apoptosis induced by arsenite is prevented by low concentrations of mitochondrial ascorbic acid with hardly any effect mediated by the cytosolic fraction of the vitamin, BioFactors, (In Press).

Legends to the figures

Fig. 1. Sub-cellular localization of SVCT2 in U937 cells. (A-E) Co-localization of anti-SVCT2 immunoreactivity with a mitochondrial fluorescent probe (MitoTracker Red CMXRos) in U937 cells. Representative fluorescence images of cells double stained for SVCT2 (green, A) and mitochondria (red, B). In the merged images, the regions containing both MitoTracker Red CMXRos and FITC fluorescence appear yellow (C). (D) Co-localisation analysis and quantification performed using Image J software where background and threshold were set, generating a co-localization image (co-localized pixels in white). (E) The Pearson's (PC) and Manders' (M1 and M2) overlap coefficients represented as the average of ten individual cells. (F) Mitochondrial fractions obtained from two different lots of untreated U937 cells were processed for Western blot analysis using antibodies against SVCT2. Blots were re-probed for HSP-60. Similar outcomes were obtained in experiments using two additional cell preparations (not shown). Mitochondria were isolated by a differential centrifugation procedure (Method 1) or by sucrose gradient centrifugation (Method 2). (G) U937 cells were homogenized and fractionated by differential centrifugation and the different fractions (N: nuclear fraction; M: mitochondria; ER: endoplasmic reticulum; PM: plasma membranes enriched fraction; C: cytoplasmic fraction) were processed for Western blot analysis using the following antibodies: anti-SVCT2, anti-calnexin for ER, anti-lamin A for N, anti-cytochrome c for M, anti-GLUT3 for PM. Blots shown are representative of 2 separate experiments with similar outcome.

Fig. 2. Kinetic properties of mitochondrial SVCT2. (A) Time-dependence of AA accumulation in isolated mitochondria exposed to 30 μM ^{14}C-AA in MB. (B) AA content in isolated mitochondria exposed to 0–60 μM ^{14}C-AA in MB. (C) Eadie-Hofstee plot of the data in B. (D) AA content in isolated mitochondria exposed to 0-1.5 mM ^{14}C-AA/AA in IB. (E) Eadie-Hofstee plot of the data in D. (F) AA uptake in isolated mitochondria exposed to 30 μM AA at different pH values in IB.

Fig. 3. Ascorbic acid transport in Raw 264.7 and U937 cells. (A) Eadie-Hofstee plot of the concentration-response curve for AA transport in Raw 264.7 cells. Inset (a): Raw 264.7 cell lysates were processed for Western blot analysis using antibodies against SVCT1 and SVCT2. Inset (b): AA content in Raw 264.7 cells exposed to 0-100 μM ^{14}C-AA in EB. (B) Eadie-Hofstee plot of the concentration-response curve for AA transport in U937 cells. Inset (a): U937 cell lysates were processed for Western blot analysis using antibodies against SVCT1 and SVCT2. Inset (b): AA content in U937 cells exposed to 0-100 μM AA in EB. (C) AA uptake in Raw 264.7 cells exposed

to 30 μM AA at different pH values in EB. Values are means, with standard deviations calculated from at least three separate experiments.

Fig. 4. Na^+-dependence of ascorbic acid transport in mitochondria isolated from U937 cells and in intact Raw 264.7 cells. (A) Effect of increasing Na^+ concentrations on ^{14}C-AA (30 μM) uptake in isolated U937 cell mitochondria bathed in MB. Inset: Hill plot of the data in A. (B) Effect of increasing Na^+ concentrations on ^{14}C-AA (30 μM) uptake in isolated U937 cell mitochondria bathed in IB. Inset: Hill plot of the data in B. (C) Effect of increasing Na^+ concentrations on AA (30 μM) uptake in intact Raw 264.7 cells bathed in EB. Inset: Hill plot of the data in C. Values are means, with standard deviations calculated from at least three separate experiments.

Fig. 5. Ca^{++} and/or Mg^{++}-dependence of ascorbic acid transport in intact Raw 264.7 cells, U937 cells and mitochondria isolated from U937 cells. (A) Raw 264.7 and U937 cells were exposed to ^{14}C-AA (30 μM) in EB manipulated as indicated in the figure. AA uptake was then determined. (B) Mitochondria isolated from U937 cells were exposed to ^{14}C-AA (30 μM) in MB manipulated as indicated in the figure and then analysed for AA accumulation. Values are means, with standard deviations calculated from at least three separate experiments.

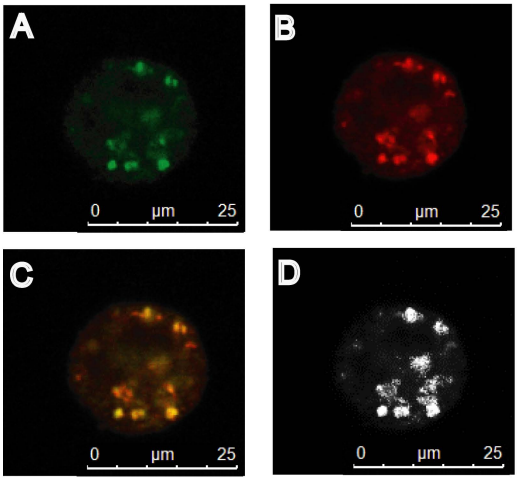
A
B
C
D
0 µm 25

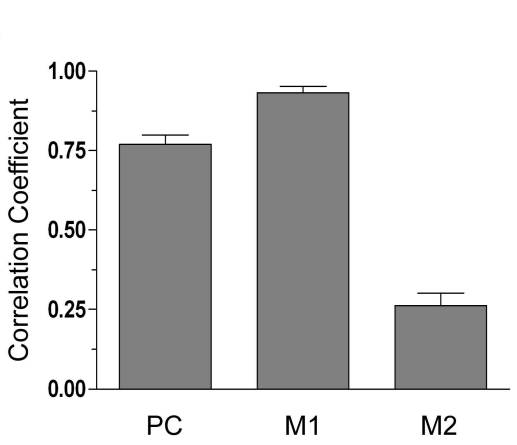
E
Correlation Coefficient
1.00
0.75
0.50
0.25
0.00
PC
M1
M2

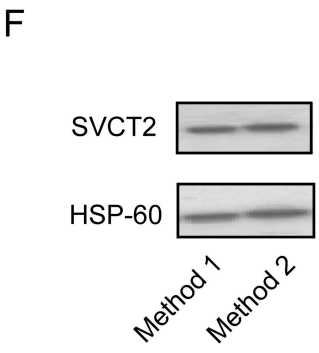
F
SVCT2
HSP-60
Method 1
Method 2

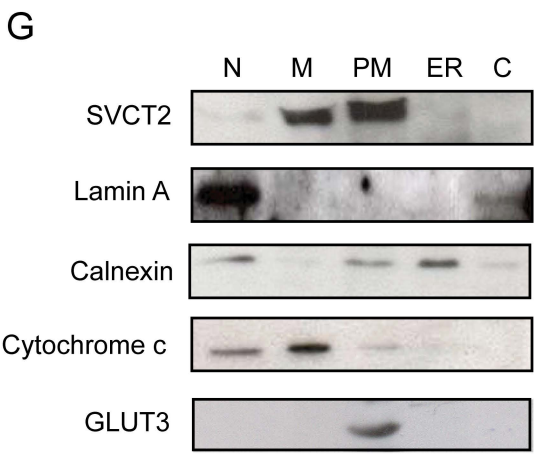
G
N
M
PM
ER
C
SVCT2
Lamin A
Calnexin
Cytochrome c
GLUT3

Figure 1

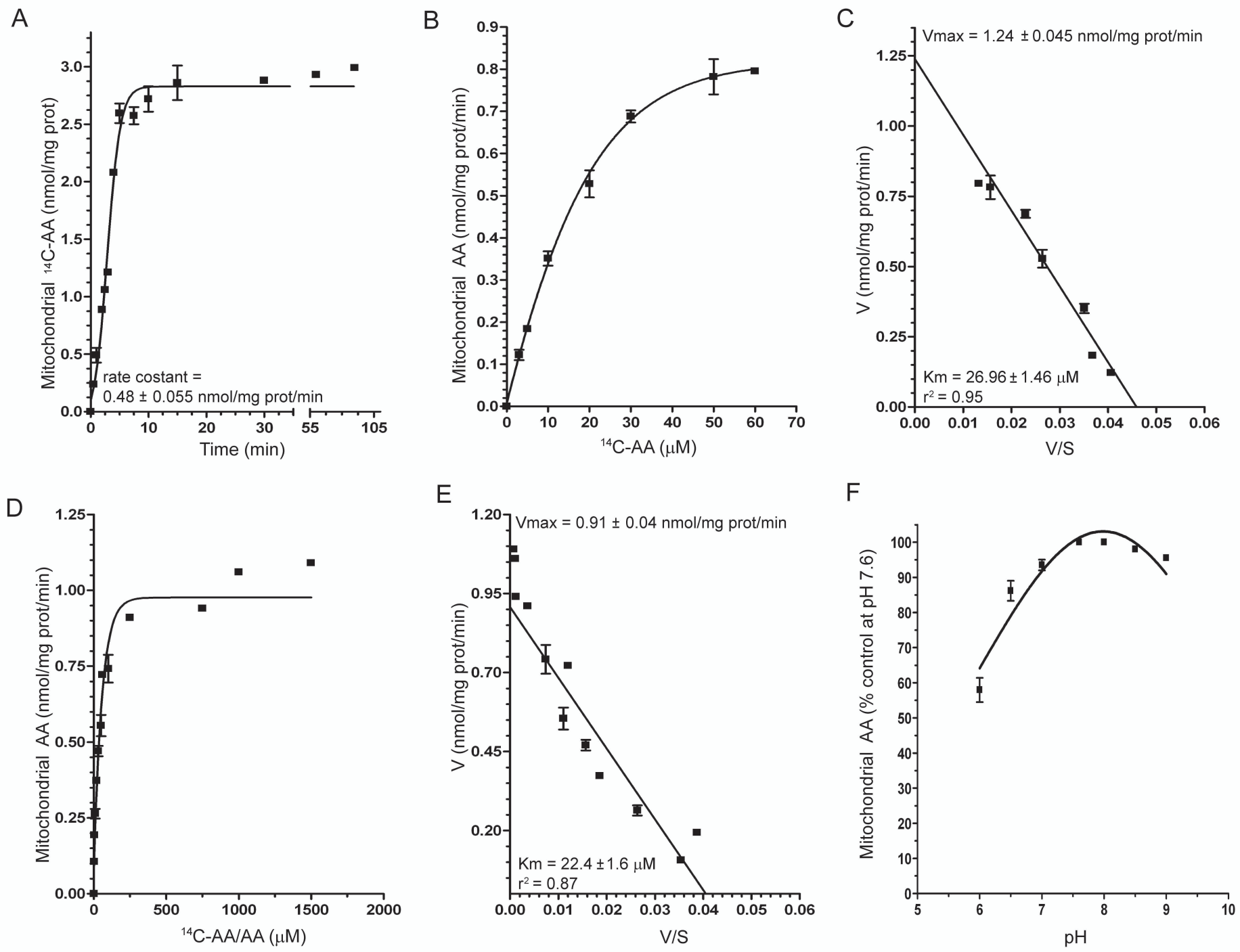
A
Mitochondrial ¹⁴C-AA (nmol/mg prot)
rate costant =
0.48 ± 0.055 nmol/mg prot/min
Time (min)
B
Mitochondrial AA (nmol/mg prot/min)
¹⁴C-AA (μM)
C
Vmax = 1.24 ± 0.045 nmol/mg prot/min
V (nmol/mg prot/min)
Km = 26.96 ± 1.46 μM
r² = 0.95
V/S
D
Mitochondrial AA (nmol/mg prot/min)
¹⁴C-AA/AA (μM)
E
Vmax = 0.91 ± 0.04 nmol/mg prot/min
V (nmol/mg prot/min)
Km = 22.4 ± 1.6 μM
r² = 0.87
V/S
F
Mitochondrial AA (% control at pH 7.6)
pH

Figure 2

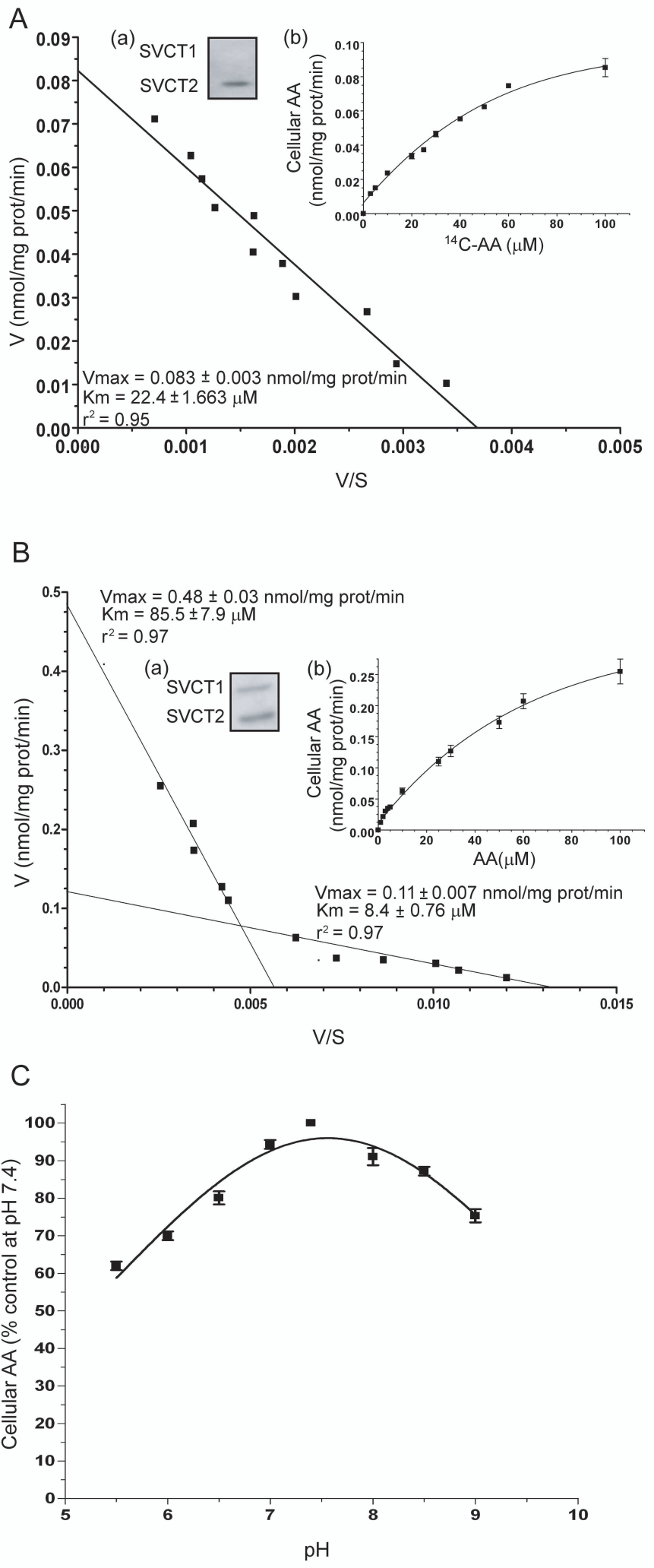
A
(a)
SVCT1
SVCT2
(b)
Cellular AA (nmol/mg prot/min)
^{14}C-AA (μM)
V (nmol/mg prot/min)
Vmax = 0.083 ± 0.003 nmol/mg prot/min
Km = 22.4 ± 1.663 μM
r^2 = 0.95
V/S
B
Vmax = 0.48 ± 0.03 nmol/mg prot/min
Km = 85.5 ± 7.9 μM
r^2 = 0.97
(a)
SVCT1
SVCT2
(b)
Cellular AA (nmol/mg prot/min)
AA(μM)
V (nmol/mg prot/min)
Vmax = 0.11 ± 0.007 nmol/mg prot/min
Km = 8.4 ± 0.76 μM
r^2 = 0.97
V/S
C
Cellular AA (% control at pH 7.4)
pH

Figure 3

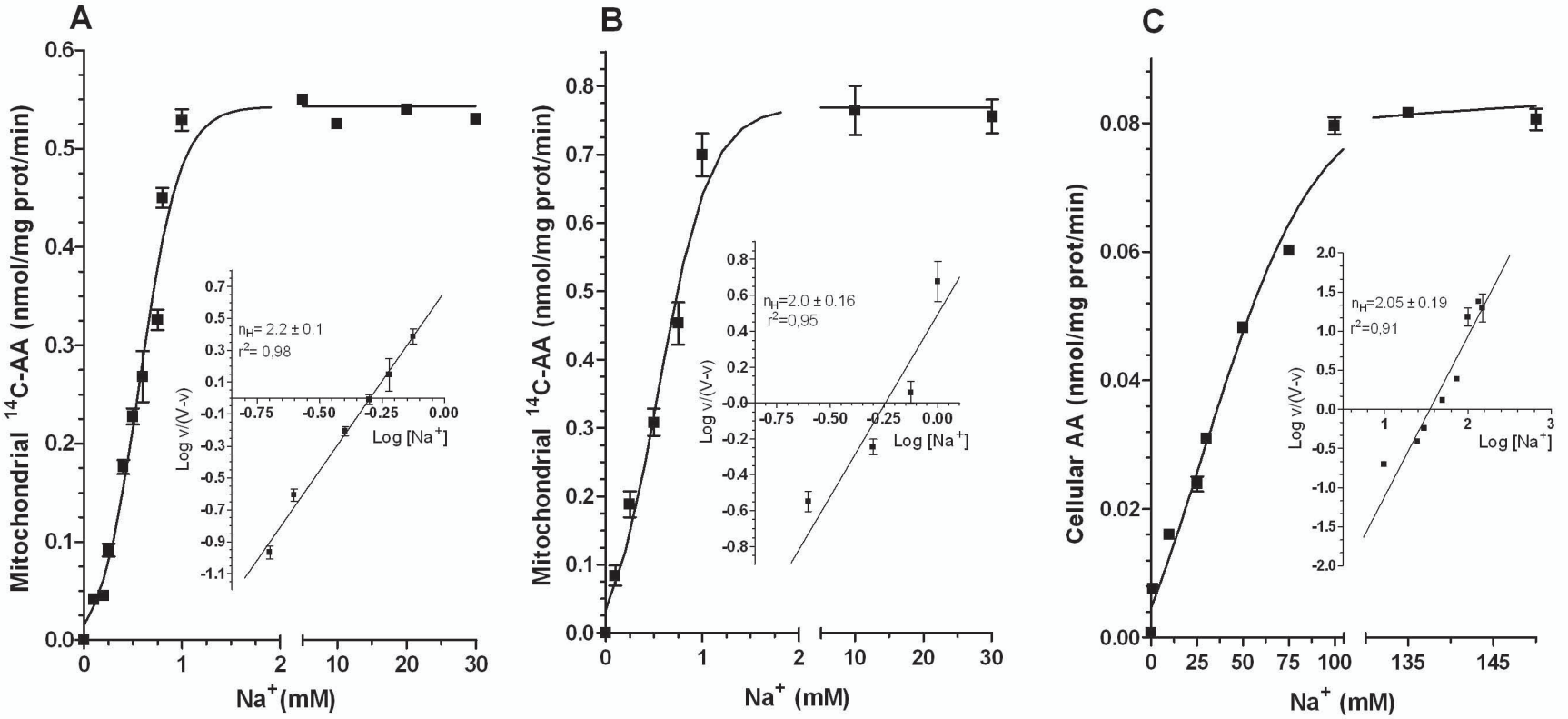
A
Mitochondrial ^{14}C-AA (nmol/mg prot/min)
Na$^+$(mM)
n_H= 2.2 ± 0.1
r^2= 0,98
Log v/(V-v)
Log [Na$^+$]
B
Mitochondrial ^{14}C-AA (nmol/mg prot/min)
Na$^+$ (mM)
n_H=2.0 ± 0.16
r^2=0,95
Log v/(V-v)
Log [Na$^+$]
C
Cellular AA (nmol/mg prot/min)
Na$^+$ (mM)
n_H=2.05 ± 0.19
r^2=0,91
Log v/(V-v)
Log [Na$^+$]

Figure 4

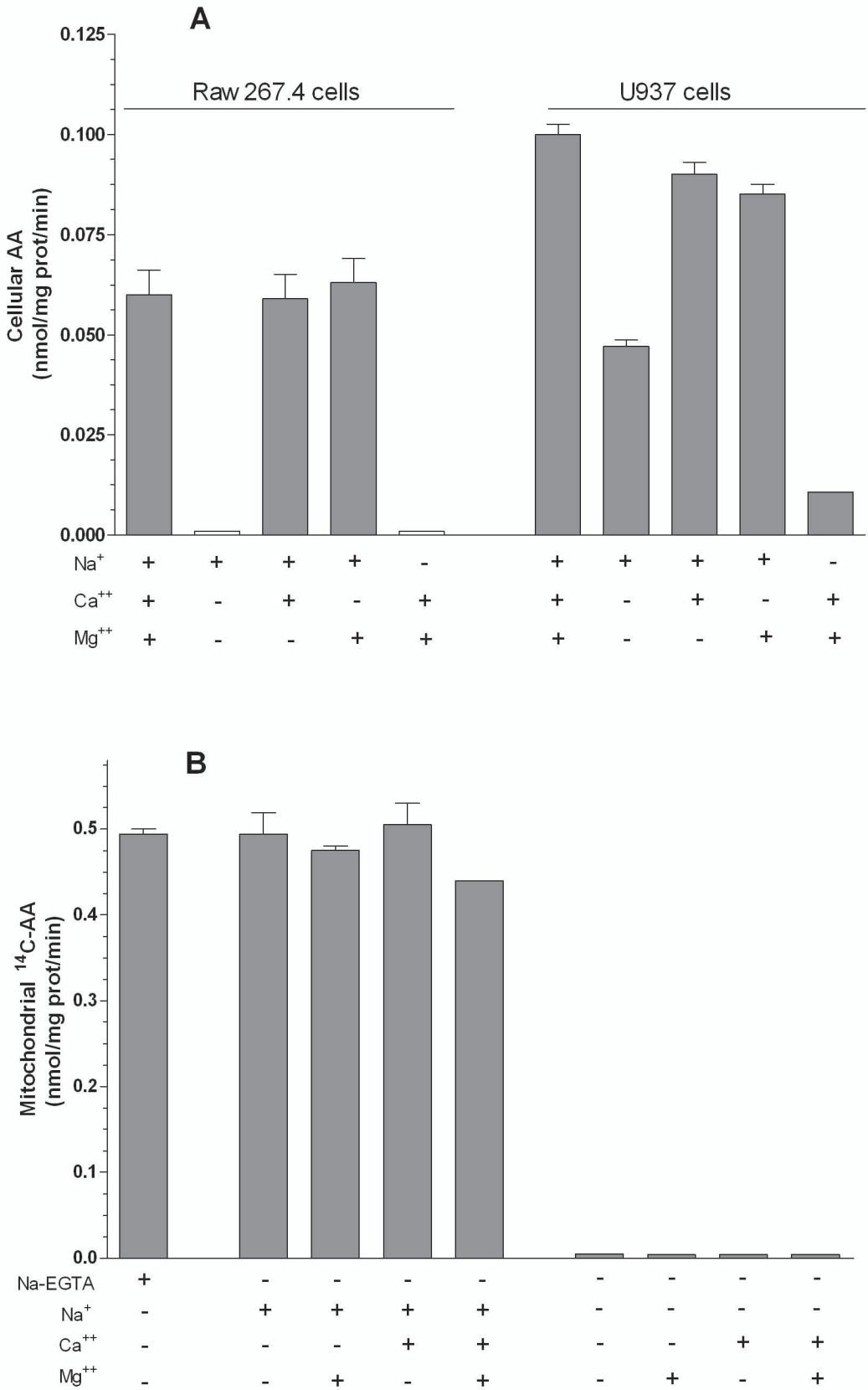
A
Raw 267.4 cells
U937 cells
Cellular AA
(nmol/mg prot/min)
0.125
0.100
0.075
0.050
0.025
0.000
Na+
Ca++
Mg++
B
Mitochondrial 14C-AA
(nmol/mg prot/min)
0.5
0.4
0.3
0.2
0.1
0.0
Na-EGTA
Na+
Ca++
Mg++

Figure 5